The Cryosphere Discuss., 9, 4019–4042, 2015
www.the-cryosphere-discuss.net/9/4019/2015/
doi:10.5194/tcd-9-4019-2015
© Author(s) 2015. CC Attribution 3.0 License.

The Cryosphere Discussions
Open Access

This discussion paper is/has been under review for the journal The Cryosphere (TC). Please refer to the corresponding final paper in TC if available.

Tropical and mid-latitude forcing of continental Antarctic temperatures

C. S. M. Turney[1,2], C. J. Fogwill[1,2], A. Klekociuk[3,4], T. D. van Ommen[3,4], M. A. J. Curran[3,4], A. D. Moy[3,4], and J. G. Palmer[1,2]

[1]Climate Change Research Centre, University of New South Wales, Sydney, Australia
[2]School of Biological, Earth and Environmental Sciences, University of New South Wales, Sydney, Australia
[3]Australian Antarctic Division, 203 Channel Highway, Kingston 7050, Tasmania, Australia
[4]Antarctic Climate and Ecosystems Cooperative Research Centre, University of Tasmania, Private Bag 80, Hobart 7001, Tasmania, Australia

Received: 12 June 2015 – Accepted: 30 June 2015 – Published: 30 July 2015

Correspondence to: C. S. M. Turney (c.turney@unsw.edu.au)

Published by Copernicus Publications on behalf of the European Geosciences Union.

Abstract

Future changes in atmospheric circulation and associated modes of variability are a major source of uncertainty in climate projections. Nowhere is this issue more acute than across the mid- to high-latitudes of the Southern Hemisphere (SH) which over the last few decades has experienced extreme and regional variable trends in precipitation, ocean circulation, and temperature, with major implications for Antarctic ice melt and surface mass balance. Unfortunately there is a relative dearth of observational data, limiting our understanding of the driving mechanism(s). Here we report a new 130-year annually-resolved record of δD – a proxy for temperature – from the South Geographic Pole where we find a significant influence from extra-tropical pressure anomalies which act as "gatekeepers" to the meridional exchange of air masses. Reanalysis of global atmospheric circulation suggests these pressure anomalies play a considerably larger influence on mid- to high-latitude SH climate than hitherto believed, modulated by the tropical Pacific Ocean. Our findings suggest that future increasing tropical warmth will strengthen meridional circulation, exaggerating current trends, with potentially significant impacts on Antarctic surface mass balance.

1 Introduction

Uncertainty surrounding future changes in atmospheric circulation is exacerbated in the Southern Hemisphere (SH) by the acutely short baseline of observations available only since the onset of continuous monitoring during the mid-20th Century and satellite era (post-1979) (Bracegirdle et al., 2015; Delworth and Zeng, 2014; Hobbs and Raphael, 2010; Marshall, 2003), despite the extreme and often contrasting trends in precipitation, ocean circulation and temperature (Gille, 2014), and Antarctic ice melt (Rye et al., 2014) which it has experienced in recent decades. In the high latitudes of the SH, the limited available data suggest opposing trends over the last few decades; while the Peninsula and West Antarctic provide strong evidence for surface

TCD
9, 4019–4042, 2015

warming (up to 2.5 °C since 1950) (Ding et al., 2011), observations and reanalysis data have provided contrasting trends over continental East Antarctica (Jones and Lister, 2014). A potentially confounding factor is the pronounced temperature inversion that exists over much of the high altitude plateau for most of the year (up to 10 °C over 30 m) (Hudson and Brandt, 2005), making the interpretation of surface reanalysis data problematic (Fréville et al., 2014). In marked contrast, radiosonde observations obtained through the upper atmosphere appear to provide a more robust signal, with pronounced warming observed across the mid-troposphere (centred on 650 hPa) during all seasons above the interior of East Antarctica, independent of the trends at the surface but limited to the last five decades (Screen and Simmonds, 2012; Turner et al., 2006).

Previous studies on Antarctic climate have suggested a significant low- and mid-latitude influence (Ding et al., 2011; Jouzel et al., 1983; Screen and Simmonds, 2012; Shaheen et al., 2013). For instance, an early study at the South Pole suggested snow δD closely mirrored the Pacific Decadal Oscillation over the previous century (Ekaykin et al., 2004). More recently, a relationship between surface temperature increases over West Antarctica, global sea surface temperature (SST), and atmospheric circulation has recently been identified (Ding et al., 2011), implying that recent warming may be coupled to the tropical Pacific. Records extending the mid-troposphere temperature record (Screen and Simmonds, 2012; Turner et al., 2006) are therefore needed to better understand the driving mechanism(s) of warming over the continent.

Fortunately, clear-sky precipitation (or diamond dust) – the isotopic signal of which preserves the temperature during formation in the mid-troposphere – dominates the total precipitation over much of the continental interior (Casey et al., 2014; Ekaykin et al., 2004; Hou et al., 2007); unlike coastal areas where different precipitation sources contribute to significant amounts of accumulation, diamond dust is continuously formed in the low atmosphere on the plateau during clear days, where most of the crystals are generated in the relatively moist upper part of the surface inversion (approximately 600–700 hPa) (Ekaykin et al., 2004; Fujita and Abe, 2006; Walden et al., 2003). During these precipitation events, thick plates/short column crystals < 150 µm are commonly observed in the South Pole atmosphere (Kikuchi and Hogan, 1978, 1976; Walden et al., 2003), often producing optical effects, such as halos. Crucially, although the quantities of this type of precipitation on a daily basis can be relatively low (Bromwich, 1988; Massom et al., 2004), estimates suggest that over a year diamond dust accounts for 50 to 91 % of accumulation on the plateau, including the South Pole (Casey et al., 2014; Ekaykin et al., 2004; Fujita and Abe, 2006; Hou et al., 2007). Diamond dust on the plateau therefore offers an opportunity to investigate long-term forcing of Antarctic temperatures, supplementing radiosonde data in the region.

2 Methods

In January 2012 a 2-metre snow pit was dug and contiguous snow samples were taken at 5 cm intervals at the South Geographic Pole (Fig. 1). The snow pit was extended to 7 m depth by a snow core (sub-sampled at 2.5 cm) obtained using a 7.5 cm diameter Kovacs corer (hand cored). δD analysis on the samples was undertaken on an IsoPrime mass spectrometer at the Antarctic Climate and Ecosystems Cooperative Research Centre (University of Tasmania). In addition, sodium (Na^+), magnesium (Mg^{2+}), non-sea salt sulfate ($nssSO_4^{2-}$) and methanesulphonic acid (MSA) were also measured; Mg^{2+} and MSA data not shown. To develop a chronology on the core, sodium (peaking mid-winter) (Ferris et al., 2011) and δD (peaking mid-summer; taken here as January) (Jouzel et al., 1983) were used to identify annual layers (Fig. 2) using Linage in the software programme *Analyseries* (Paillard et al., 1996). The identification of the 1991 Mount Pinatubo and Cerro Hudson eruptions in the 1992–1993 South Geographic Pole core is consistent with previous studies (Cole-Dai and Mosley-Thompson, 1999; Ferris et al., 2011).

The 2012 core overlapped with a previously reported δD sequence for the South Geographic Pole across the year CE 1977 (Jouzel et al., 1983). The chronology for the older part of the sequence was based on visible stratigraphic observations, deuterium

CC BY

maxima, tritium and β peaks (the latter across the 1960s and 1970s) (Jouzel et al., 1983), providing a robust chronology back to 1887 (Fig. S1 in the Supplement). To investigate multidecadal trends and reduce the impact of any missing years in the new combined South Pole record, we used a 30-year smoothing through the sequence.

3 Results and discussion

The resulting composite record of temperature-sensitive δD therefore extends the radiosonde record back before 1961 (Screen and Simmonds, 2012; Turner et al., 2006) (Fig. 3). Prior to the 1940s we observe high inter-annual variability but with relatively stable long-term (30-year running mean) δD values, implying temperatures did not vary significantly in the mid-troposphere over this period. From the 1940s through to the 1960s, however, we identify a trend to lower temperatures (depleted deuterium content) that was reversed in the late 1960s and sustained up to present day.

To explore the potential role of SH circulation on temperatures over the South Geographic Pole and the wider Antarctic continent (equatorwards of 65° S), we investigated monthly average reanalysis data from ERA-Interim (Dee et al., 2011) and the Twentieth Century Reanalysis (20CR) (Compo et al., 2011) (see Supplement). For ERA-Interim, we find that on average the largest areas of significant positive temperature anomalies in the Antarctic are associated with negative surface pressure anomalies (Fig. 4a) extending up to 700 hPa (Fig. S2) in specific regions, most notably over the southeastern Indian Ocean, southwestern Pacific (and to a lesser extent in the southwestern Atlantic) of the SH, and also in the eastern tropical Pacific (similar responses are also observed where comparisons are made poleward of 55 and 75° S; data not shown). In contrast, large areas of significant negative Antarctic temperature anomalies are associated with months of positive pressure anomalies in similar regions but have a stronger association with the southern Indian Ocean and the central-eastern equatorial Pacific (Fig. 4b); indeed the southwestern Pacific and southwestern Atlantic centres are relatively weak in this phase. There is a less pronounced connection

TCD
9, 4019–4042, 2015

Discussion Paper | Discussion Paper | Discussion Paper | Discussion Paper |

between the Antarctic and lower latitudes in the other two anomaly combinations (temperature and pressure anomalies either both positive or both negative; Fig. S3). Patterns consistent with those shown in Figs. 4, S2, and S3 were also obtained using 20CR (not shown).

The distribution of the key southern mid-latitude centres in Fig. 4 may be related to the pressure anomaly field of the Southern Annular Mode (SAM), defined as the pressure difference between the mid-latitudes (around 40° S) and the Antarctic continent (65° S) (Marshall, 2003). Long-term trends in sea level pressure were extracted from 20th Century Reanalysis (Compo et al., 2011). Analysis of the distribution of extremes in the 10th and 90th percentiles in the southern Indian Ocean and southwest Pacific deseasonalised MSLP (1979 to present day) indicate the distribution of anomalies is across the year and not skewed to a particular month or season (Fig. 5). This is in contrast to the marked winter-spring asymmetry focused on the southwest Pacific that is associated with SAM (Fogt et al., 2012). Curiously, while SAM is known to exhibit some spatial and temporal asymmetry (Fogt et al., 2012), the low pressure anomalies associated here with warming over the South Geographic Pole and wider Antarctica may be associated with the zonal wave-3 pattern (ZW3) (Raphael, 2004) which plays a significant role in meridional flow across 45–55° S on interannual to decadal timescales (Steig et al., 2009). ZW3 has been linked to changing sea ice concentration in the Southern Ocean (Raphael, 2007), the delivery of rainfall to southwest Australia (van Ommen and Morgan, 2010) and recent warming over West Antarctica (Steig et al., 2009). Estimates obtained across the period of satellite observations (post-1979) suggest ZW3 explains some 8 % of SH circulation but hemispherically-averaged reconstructions only extend back to the 1960s (Raphael, 2004), hampering our understanding of its significance on multi-decadal timescales. Long-term changes in ZW3 and its influence on the SH remain highly uncertain, with limited observational data in a marine-dominated realm. Recent work has suggested ZW3 provides a mechanism for the meridional exchange of air masses, implying a strengthening since the 1970s (Schneider et al., 2004; van Ommen and Morgan, 2010), a trend coupled models struggle to reproduce (Holland and Raphael, 2006; Landrum et al., 2012; Steig et al., 2009).

We observe fields at 700 hPa composited for 10th percentile (negative) surface pressure anomalies in the southeastern Indian Ocean (panels a–e of Figs. 6 and S4) and southwestern Pacific Ocean (panels a–e of Figs. 7 and S5) are associated with an increase in geopotential height (GPH) over the Antarctic continent. Both the ERA (Figs. 6 and 7) and 20CR (Figs. S4 and S5) generate similar patterns, providing confidence that large scale processes are being appropriately captured. By examining the meridional mass streamfunction (Fig. 7), we find that in comparison with the situation in the intermediate state, the negative anomaly state shows a weakening (reduced volume) of the Polar cell and a strengthening (increased volume) of the Ferrel cell (particularly on the poleward side of the cell), consistent with increased poleward heat transport. In marked contrast, the opposite pattern is observed with positive pressure anomalies in the mid-latitudes, with a stronger Polar cell (particularly with the SIO region) and weaker Ferrel cell (most marked with the SWP), suggesting a greater dynamical barrier to poleward heat transport.

To explore whether this relationship has changed over time (pre-satellite era) we undertook wavelet coherence analysis between the Pacific and Indian Ocean pressure anomalies as extracted from the 20CR with our newly obtained South Geographic Pole δD record (Fig. 9). Focusing on the second half of the twentieth century (considered to have more reliable reconstructive ability over the mid latitudes of the SH) (Compo et al., 2011), we observe a significant shift in the dominance of the different pressure anomalies. During the period of the 1940s through to the late 1960s, low-pressure anomalies centered on the south Indian Ocean lead warming over the South Pole across the periodicity 6–12 years (arrows pointing up and to the left); in the southwest Pacific, the pressure anomalies did not lead but were in antiphase over the same periodicity but did not lead (arrows pointing to the left). But in the 1970s, this coherence ended in the south Indian Ocean and the leading pressure anomaly switched to the southwest Pacific (arrows pointing up), paralleling the 30-year trend in these

CC BY

sectors (Fig. 3), suggesting a switch in the dominant influence of different regions over continental Antarctic temperatures. Further work is required to extend the observational record of the mid-latitudes beyond the mid-1940s.

Intriguingly, the spatial plots of pressure anomalies vs. Antarctic temperature suggest the tropical Pacific may play a role. During positive pressure anomalies, the eastern Pacific also experiences higher sea level pressure and is associated with cooling over continental East Antarctica (Fig. 4b). Conversely, with increasing El Niño–Southern Oscillation (ENSO) variance (Fig. 3) (McGregor et al., 2013), the southwest Pacific pressure anomaly apparently weakens (Fig. 4a). Previous studies have demonstrated tropical Pacific variability has a significant influence on the mid- to high-latitudes (Turner, 2004; Vance et al., 2012), particularly over the west Antarctic where atmospheric teleconnections are relatively strong (Bromwich et al., 2000; Ding et al., 2011). Whilst the southwest Pacific pressure anomaly exhibits a significant relationship with annual average GPH in the tropical west Pacific (Fig. 7), absolute differences in the tropics are relatively small (Fig. 8) and may be masked by seasonal changes. To investigate this more fully, we undertook seasonal correlations between changes in southwest Pacific pressure, GPH (700 hPa) and sea surface temperatures across the period 1979–2013 (Fig. 10). We observe a significant inverse relationship with the tropical west Pacific between September and May but find no significant correlations during the Austral winter (June to August). Specifically, we find low pressure over the southwest Pacific is associated with the centres of low pressure in the south Indian Ocean and the southwest Atlantic Ocean, high temperatures in the Amundsen Sea and the central and east tropical Pacific, and relatively high pressure over the tropical west Pacific (Fig. 10). The seasonal and geographical nature of this relationship is consistent with a tropical Pacific (ENSO) (Collins et al., 2010) influence over surface Antarctic temperatures via the southwest Pacific.

Previous workers have suggested central tropical Pacific temperatures can generate a Rossby wave response that may explain winter warming over western Antarctica (Ding et al., 2011). Our results suggest a similar response to ENSO-forcing that extends

CC BY

from the tropical west Pacific down to the Antarctic via the southwest Pacific during the summer (Fig. 10). Circulation changes associated with El Niño appear to lead to a relative weakening of the pressure anomalies in the southwest Pacific Ocean (Fig. 3), strengthening the Ferrel cell while weakening the Polar cell (Fig. 8). In contrast, the negative pressure anomaly in the tropical east Pacific identified in Fig. 4b is consistent with the La Niña-like conditions and an intensified Walker Cell circulation, increasing atmospheric pressure in the east. Importantly, the recently observed increase in ENSO variability over the last three decades (with an associated increase in temperature over the Antarctic) implies the recent dominance of the southwest Pacific pressure anomaly over meridional air exchange in the mid-latitudes (Fig. 3) is exceptional in the context of the past six centuries (McGregor et al., 2013). If correct, the observed links to Antarctic temperatures suggest long-term changes in the tropics may in fact play a significant role in driving high-latitude temperatures (Figs. 4 and 10), with potential implications for past climate states (Pedro et al., 2011; Visser et al., 2003).

4 Conclusions

By extending historical observations over the South Pole and in combination with reanalysis products we find that meridional circulation changes associated with centres of pressure anomalies are part of a broader change observed over recent decades. Of particular note is the marked decrease in rainfall in southwest Australia since the 1970s. Our results demonstrate this trend is part of a hemispheric pattern of alternating northerly and southerly airflow linked to changes in the southwest Pacific and the tropical Pacific. We explore possible teleconnections via a strengthening of the Ferrel Cell and weakening Polar Cell. Comparison of 30-year running means of isotopic and climate datasets suggest the continuing trend to lower pressure anomalies in the southwest Pacific – with largely stable values in the Indian Ocean – are consistent with increased ENSO variability, implying precipitation will continue to decline in southwest

Australia if El Niños become more frequent, and lead to greater warming over the Antarctic, potentially impacting the future surface mass balance.

The Supplement related to this article is available online at doi:10.5194/tcd-9-4019-2015-supplement.

Acknowledgements. The authors thank the Australian Research Council for their financial support (FL100100195; LP120200724, DP130104156 and FT120100004). We are extremely grateful to the support in the field provided by Antarctic Logistics and Expeditions (ALE) who made this work possible. Many thanks to J. Jouzel for providing the data from previous work at South Pole.

References

Bracegirdle, T., Bertler, N., Carleton, A., Ding, Q., Fogwill, C., Fyfe, J., Hellmer, H., Karpechko, A., Kusahara, K., and Larour, E.: A multi-disciplinary perspective on climate model evaluation for Antarctica, B. Am. Meteorol. Soc., doi:10.1175/BAMS-D-15-00108.1, online first, 2015.

Bromwich, D.: Snowfall in high southern latitudes, Rev. Geophys., 26, 149–168, 1988.

Bromwich, D. H., Rogers, A. N., Kållberg, P., Cullather, R. I., White, J. W. C., and Kreutz, K. J.: ECMWF analyses and reanalyses depiction of ENSO signal in Antarctic precipitation, J. Climate, 13, 1406–1420, 2000.

Casey, K., Fudge, T., Neumann, T., Steig, E., Cavitte, M., and Blankenship, D.: The 1500 m South Pole ice core: recovering a 40 ka environmental record, Ann. Glaciol., 55, 137–146, 2014.

Cole-Dai, J. and Mosley-Thompson, E.: The Pinatubo eruption in South Pole snow and its potential value to ice-core paleovolcanic records, Ann. Glaciol., 29, 99–105, 1999.

Collins, M., An, S.-I., Cai, W., Ganachaud, A., Guilyardi, E., Jin, F.-F., Jochum, M., Lengaigne, M., Power, S., Timmermann, A., Vecchi, G., and Wittenberg, A.: The impact of global warming on the tropical Pacific Ocean and El Nino, Nat. Geosci., 3, 391–397, 2010.

TCD

9, 4019–4042, 2015

Tropical and mid-latitude forcing of continental Antarctic temperatures

C. S. M. Turney et al.

CC BY

Compo, G. P., Whitaker, J. S., Sardeshmukh, P. D., Matsui, N., Allan, R. J., Yin, X., Gleason, B. E., Vose, R. S., Rutledge, G., Bessemoulin, P., Brönnimann, S., Brunet, M., Crouthamel, R. I., Grant, A. N., Groisman, P. Y., Jones, P. D., Kruk, M. C., Kruger, A. C., Marshall, G. J., Maugeri, M., Mok, H. Y., Nordli, Ø., Ross, T. F., Trigo, R. M., Wang, X. L., Woodruff, S. D., and Worley, S. J.: The Twentieth Century Reanalysis Project, Q. J. Roy. Meteor. Soc., 137, 1–28, 2011.

Dee, D. P., Uppala, S. M., Simmons, A. J., Berrisford, P., Poli, P., Kobayashi, S., Andrae, U., Balmaseda, M. A., Balsamo, G., Bauer, P., Bechtold, P., Beljaars, A. C. M., van de Berg, L., Bidlot, J., Bormann, N., Delsol, C., Dragani, R., Fuentes, M., Geer, A. J., Haimberger, L., Healy, S. B., Hersbach, H., Hólm, E. V., Isaksen, L., Kållberg, P., Köhler, M., Matricardi, M., McNally, A. P., Monge-Sanz, B. M., Morcrette, J. J., Park, B. K., Peubey, C., de Rosnay, P., Tavolato, C., Thépaut, J. N., and Vitart, F.: The ERA-Interim reanalysis: configuration and performance of the data assimilation system, Q. J. Roy. Meteor. Soc., 137, 553–597, 2011.

Delworth, T. L. and Zeng, F.: Regional rainfall decline in Australia attributed to anthropogenic greenhouse gases and ozone levels, Nat. Geosci., 7, 583–587, 2014.

Ding, Q., Steig, E. J., Battisti, D. S., and Kuttel, M.: Winter warming in West Antarctica caused by central tropical Pacific warming, Nat. Geosci., 4, 398–403, 2011.

Ekaykin, A. A., Lipenkov, V. Y. A., Kuzmina, I. N., Petit, J. R., Masson-Delmotte, V., and Johnsen, S. J.: The changes in isotope composition and accumulation of snow at Vostok station, East Antarctica, over the past 200 years, Ann. Glaciol., 39, 569–575, 2004.

Ferris, D. G., Cole-Dai, J., Reyes, A. R., and Budner, D. M.: South Pole ice core record of explosive volcanic eruptions in the first and second millennia A.D., and evidence of a large eruption in the tropics around 535 A.D., J. Geophys. Res., 116, 116, D17308, doi:10.1029/2011JD015916, 2011.

Fogt, R. L., Jones, J. M., and Renwick, J.: Seasonal zonal asymmetries in the Southern Annular Mode and their impact on regional temperature anomalies, J. Climate, 25, 6253–6270, 2012.

Fréville, H., Brun, E., Picard, G., Tatarinova, N., Arnaud, L., Lanconelli, C., Reijmer, C., and van den Broeke, M.: Using MODIS land surface temperatures and the Crocus snow model to understand the warm bias of ERA-Interim reanalyses at the surface in Antarctica, The Cryosphere, 8, 1361–1373, doi:10.5194/tc-8-1361-2014, 2014.

Fujita, K. and Abe, O.: Stable isotopes in daily precipitation at Dome Fuji, East Antarctica, Geophys. Res. Lett., 33, L18503, doi:10.1029/2006GL026936, 2006.

CC BY

Gille, S. T.: Meridional displacement of the Antarctic Circumpolar Current, Philos. T. R. Soc. A, 372, 20130273, doi:10.1098/rsta.2013.0273, 2014.

Hobbs, W. and Raphael, M.: Characterizing the zonally asymmetric component of the SH circulation, Clim. Dynam., 35, 859–873, 2010.

Holland, M. and Raphael, M.: Twentieth century simulation of the Southern Hemisphere climate in coupled models. Part II: Sea ice conditions and variability, Clim. Dynam., 26, 229–245, 2006.

Hou, S., Li, Y., Xiao, C., and Ren, J.: Recent accumulation rate at Dome A, Antarctica, Chinese Sci. Bull., 52, 428–431, 2007.

Hudson, S. R. and Brandt, R. E.: A look at the surface-based temperature inversion on the Antarctic Plateau, J. Climate, 18, 1673–1696, 2005.

Jones, P. D. and Lister, D. H.: Antarctic near-surface air temperatures compared with ERA-Interim values since 1979, Int. J. Climatol., 35, 1354–1366, doi:10.1002/joc.4061, 2014.

Jouzel, J., Merlivat, L., Petit, J. R., and Lorius, C.: Climatic information over the last century deduced from a detailed isotopic record in the South Pole snow, J. Geophys. Res., 88, 2693–2703, 1983.

Kikuchi, K. and Hogan, A. W.: Snow crystal observations in summer season at Amundsen–Scott South Pole Station, Antarctica, Journal of the Faculty of Science, Hokkaido University, Series 7, Geophysics, 5, 1–20, 1976.

Kikuchi, K. and Hogan, A. W.: Properties of diamond dust type ice crystals observed in summer season at Amundsen–Scott South Pole Station, Antarctica, J. Meteorol. Soc. Jpn., 57, 180–189, 1978.

Landrum, L., Holland, M. M., Schneider, D. P., and Hunke, E.: Antarctic sea ice climatology, variability, and late Twentieth-Century change in CCSM4, J. Climate, 25, 4817–4838, 2012.

Marshall, G.: Trends in the southern annular mode from observations and reanalyses, J. Climate, 16, 4134–4143, 2003.

Massom, R. A., Pook, M. J., Comiso, J. C., Adams, N., Turner, J., Lachlan-Cope, T., and Gibson, T. T.: Precipitation over the interior East Antarctic ice sheet related to midlatitude blocking-high activity, J. Climate, 17, 1914–1928, 2004.

McGregor, S., Timmermann, A., England, M. H., Elison Timm, O., and Wittenberg, A. T.: Inferred changes in El Niño–Southern Oscillation variance over the past six centuries, Clim. Past, 9, 2269–2284, doi:10.5194/cp-9-2269-2013, 2013.

CC BY

Paillard, D., Labeyrie, L., and Yiou, P.: Macintosh program performs time-series analysis, EOS T. Am. Geophys. Un., 77, 379, doi:10.1029/96EO00259, 1996.
Pedro, J. B., van Ommen, T. D., Rasmussen, S. O., Morgan, V. I., Chappellaz, J., Moy, A. D., Masson-Delmotte, V., and Delmotte, M.: The last deglaciation: timing the bipolar seesaw, Clim. Past, 7, 671–683, doi:10.5194/cp-7-671-2011, 2011.
Raphael, M. N.: A zonal wave 3 index for the Southern Hemisphere, Geophys. Res. Lett., 31, L23212, doi:10.1029/2004GL020365, 2004.
Raphael, M. N.: The influence of atmospheric zonal wave three on Antarctic sea ice variability, J. Geophys. Res., 112, D12112, doi:10.1029/2006JD007852, 2007.
Rayner, N. A., Parker, D. E., Horton, E. B., Folland, C. K., Alexander, L. V., Rowell, D. P., Kent, E. C., and Kaplan, A.: Global analyses of sea surface temperature, sea ice, and night marine air temperature since the late nineteenth century, J. Geophys. Res., 108, 4407, doi:10.1029/2002JD002670, 2003.
Rye, C. D., Naveira Garabato, A. C., Holland, P. R., Meredith, M. P., George Nurser, A. J., Hughes, C. W., Coward, A. C., and Webb, D. J.: Rapid sea-level rise along the Antarctic margins in response to increased glacial discharge, Nat. Geosci., 7, 732–735, 2014.
Schneider, D. P., Steig, E. J., and Comiso, J. C.: Recent climate variability in Antarctica from satellite-derived temperature data, J. Climate, 17, 1569–1583, 2004.
Screen, J. A. and Simmonds, I.: Half-century air temperature change above Antarctica: Observed trends and spatial reconstructions, J. Geophys. Res., 117, D16108, doi:10.1029/2012JD017885, 2012.
Shaheen, R., Abauanza, M., Jackson, T. L., McCabe, J., Savarino, J., and Thiemens, M. H.: Tales of volcanoes and El-Niño southern oscillations with the oxygen isotope anomaly of sulfate aerosol, P. Natl. Acad. Sci. USA, 110, 17662–17667, doi:10.1073/pnas.1213149110, 2013.
Steig, E. J., Schneider, D. P., Rutherford, S. D., Mann, M. E., Comiso, J. C., and Shindell, D. T.: Warming of the Antarctic ice-sheet surface since the 1957 International Geophysical Year, Nature, 457, 459–462, 2009.
Turner, J.: The El Niño–Southern Oscillation and Antarctica, Int. J. Climatol., 24, 1–31, 2004.
Turner, J., Lachlan-Cope, T. A., Colwell, S., Marshall, G. J., and Connolley, W. M.: Significant warming of the Antarctic winter troposphere, Science, 311, 1914–1917, 2006.
van Ommen, T. D. and Morgan, V.: Snowfall increase in coastal East Antarctica linked with southwest Western Australian drought, Nat. Geosci., 3, 267–272, 2010.

Vance, T. R., van Ommen, T. D., Curran, M. A. J., Plummer, C. T., and Moy, A. D.: A millennial proxy record of ENSO and eastern Australian rainfall from the Law Dome ice core, East Antarctica, J. Climate, 26, 710–725, 2012.
Visser, K., Thunell, R., and Stott, L.: Magnitude and timing of temperature change in the Indo-Pacific warm pool during deglaciation, Nature, 421, 152–155, 2003.
Walden, V. P., Warren, S. G., and Tuttle, E.: Atmospheric ice crystals over the Antarctic Plateau in winter, J. Appl. Meteorol., 42, 1391–1405, 2003.

TCD
9, 4019–4042, 2015

CC BY

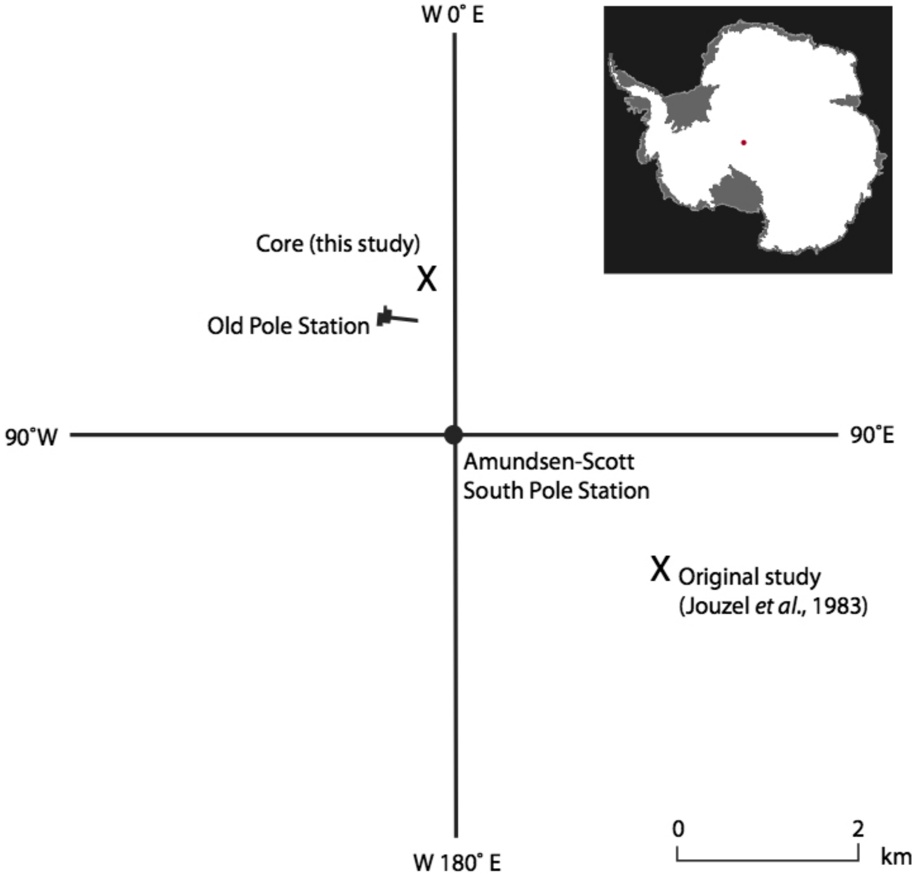

Figure 1. Location of cores investigated at the South Geographic Pole.

TCD
9, 4019–4042, 2015

CC BY

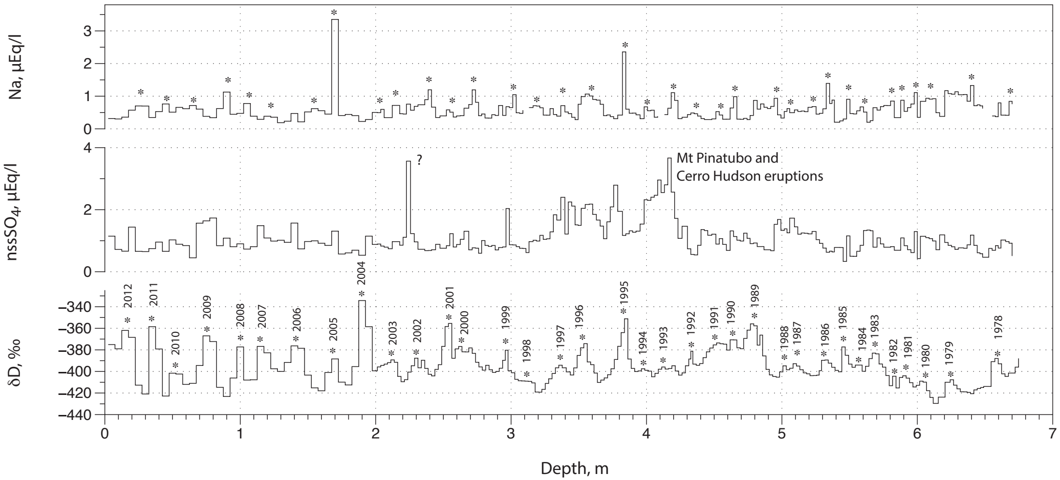

Figure 2. Annual layers identified in the South Geographic Pole core obtained in January 2012. Asterisks denote peaks in sodium (Na^+) and deuterium (δD), marking mid-winter and -summer respectively.

TCD
9, 4019–4042, 2015

CC BY

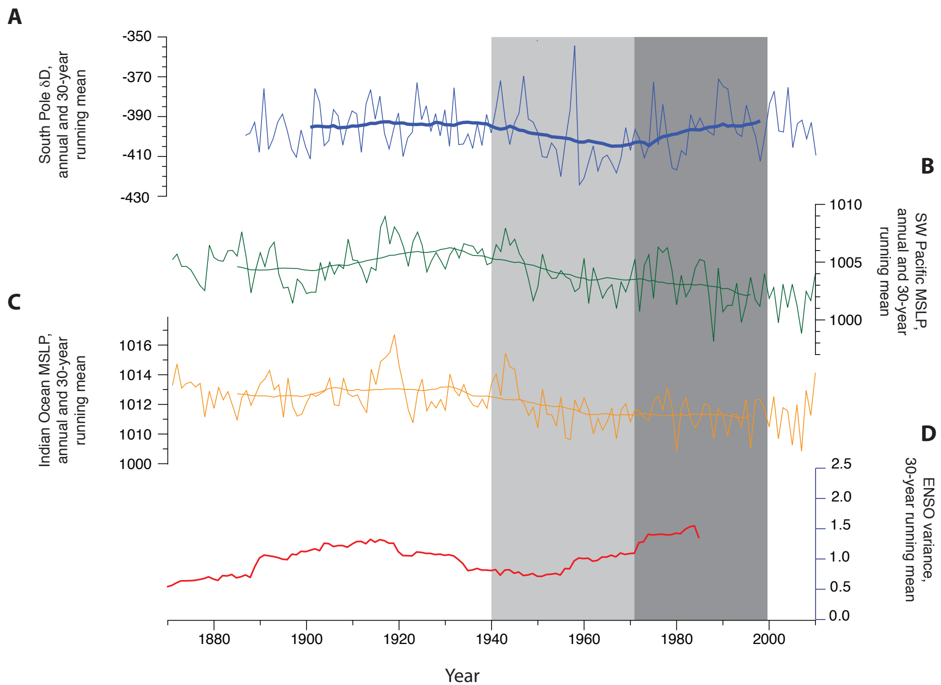

Figure 3. Annual and 30-year running mean of South Pole δD **(a)** compared to annual and 30 year running mean sea level pressure (hPa) for the southwestern Pacific (180–160° W, 55–45° S) **(b)** and southern Indian Ocean (80–100° E, 35–45° S) **(c)** extracted from 20th Century Reanalysis (Compo et al., 2011), and 30-year variance in El Niño–Southern Oscillation (McGregor et al., 2013) **(d)**. Light grey column area denotes a period of Indian Ocean MSLP dominance over Antarctic temperatures; the dark grey column denotes the period where sustained decreasing Southwest Pacific MSLP leads to warming over the South Geographic Pole.

TCD
9, 4019–4042, 2015

CC BY

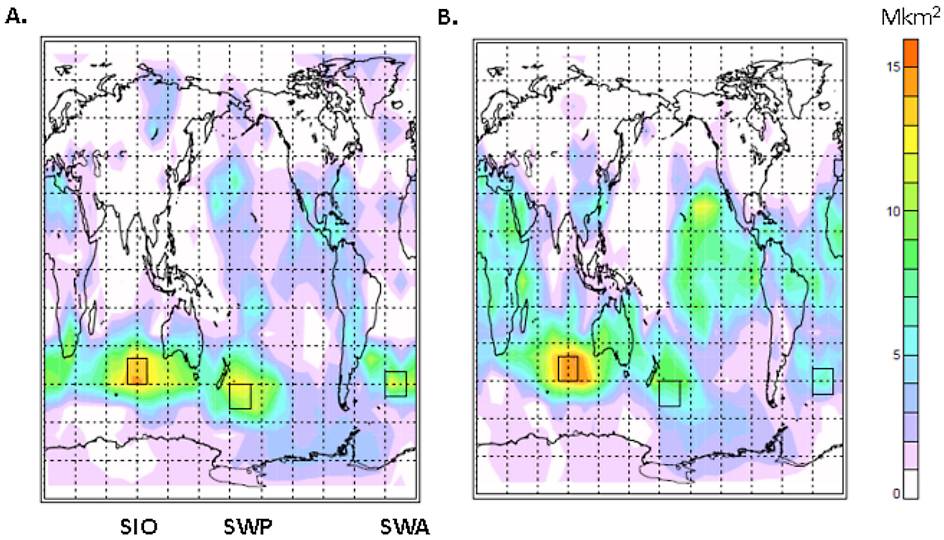

Figure 4. (a) The cumulative area of significant positive surface temperature anomalies poleward of 65° S (in million km^2) produced by compositing months having negative surface pressure anomalies (thresholded at the 10th percentile) in each 10° × 10° (longitude × latitude) box, obtained from deseasonalised monthly ERA-Interim reanalysis data for 1979–2012 (Dee et al., 2011). The three boxes define the positions referred to in the text as Southern Indian Ocean (SIO), Southwestern Pacific (SWP) and Southwestern Atlantic (SWA). Panel **(b)** shows the opposite relationship i.e. the area of negative temperature anomalies produced by compositing months of positive surface pressure anomalies (thresholded at the 90th percentile). The grid spacing is 15° in longitude and latitude. For reference, the area of the Antarctic continent is 14 million km^2 and the area poleward of 65° S is 25 million km^2.

TCD
9, 4019–4042, 2015

Tropical and mid-latitude forcing of continental Antarctic temperatures

C. S. M. Turney et al.

CC BY

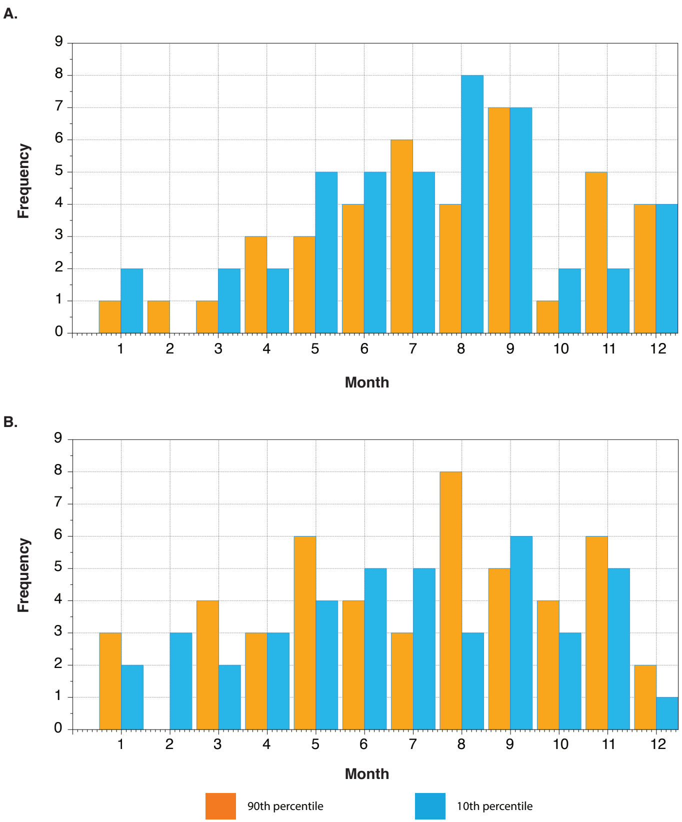

Figure 5. Distribution of 10th and 90th percentile deseasonalised surface pressure plotted for each month from 1979 to 2012 extracted from 20CR for the south Indian **(a)** and southwest Pacific **(b)** oceans. Note that anomalies occur throughout the year.

TCD
9, 4019–4042, 2015
Tropical and mid-latitude forcing of continental Antarctic temperatures
C. S. M. Turney et al.

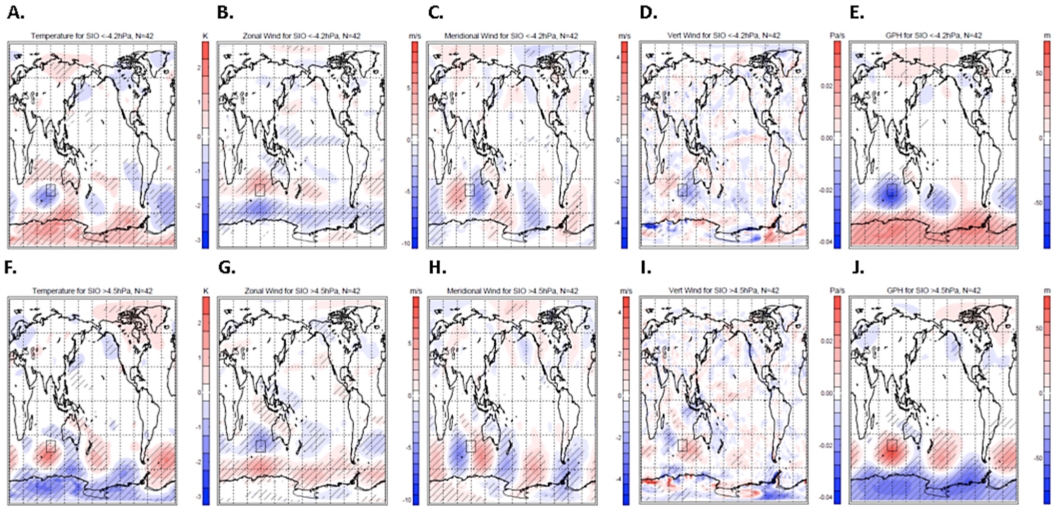

Figure 6. Composites of deseasonalised monthly ERA-Interim fields at 700 hPa for surface pressure 10th percentile (negative) and 90th percentile (positive) anomalies in the southern Indian Ocean (SIO) (80–100° E, 35–45° S) for 1979–2012 (Dee et al., 2011). Shown are temperature (**a** and **f**), zonal wind speed (**b** and **g**; positive = eastward) and meridional wind speed (**c** and **h**; positive = northward), vertical pressure wind (**d** and **i**; positive = downward) and geopotential height (**e** and **j**). The SIO surface pressure anomaly threshold and the number of months (N) contributing to each composite are shown along the top of each panel. Hatched areas denote areas of statistical significance (95 % confidence).

TCD

9, 4019–4042, 2015

Tropical and mid-latitude forcing of continental Antarctic temperatures

C. S. M. Turney et al.

CC BY

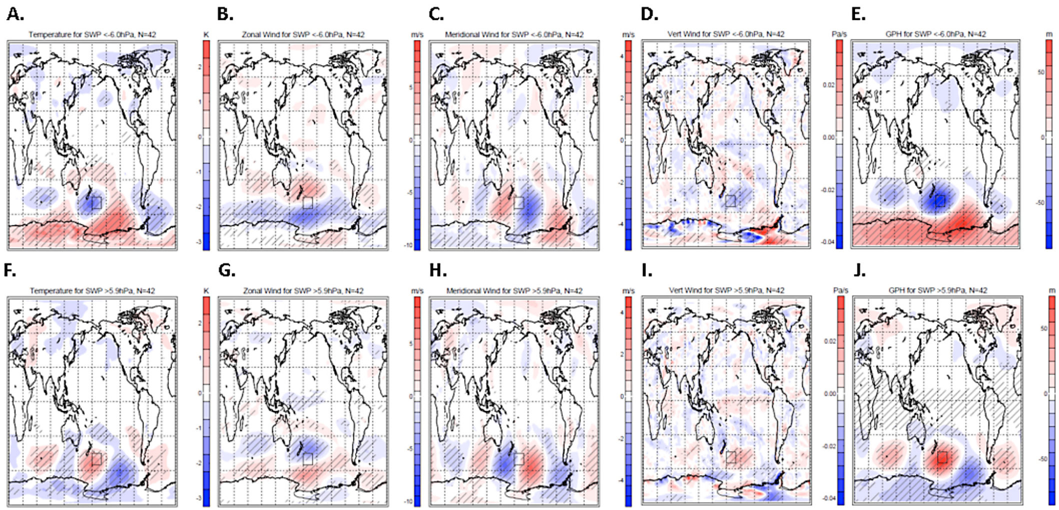

Figure 7. Composites of deseasonalised monthly ERA-Interim reanalysis fields at 700 hPa for surface pressure 10th percentile (negative) and 90th percentile (positive) anomalies in the southwestern Pacific (SWP) Ocean (180–200° E, 45–55° S) for 1979–2012 (Dee et al., 2011). Shown are temperature (**a** and **f**), zonal wind speed (**b** and **g**; positive = eastward) and meridional wind speed (**c** and **h**; positive = northward), vertical pressure wind (**d** and **i**; positive = downward) and geopotential height (**e** and **j**). The SWP surface pressure anomaly threshold and the number of months (N) contributing to each composite are shown at the top of each panel. Hatched areas denote areas of statistical significance (95 % confidence).

TCD
9, 4019–4042, 2015

CC BY

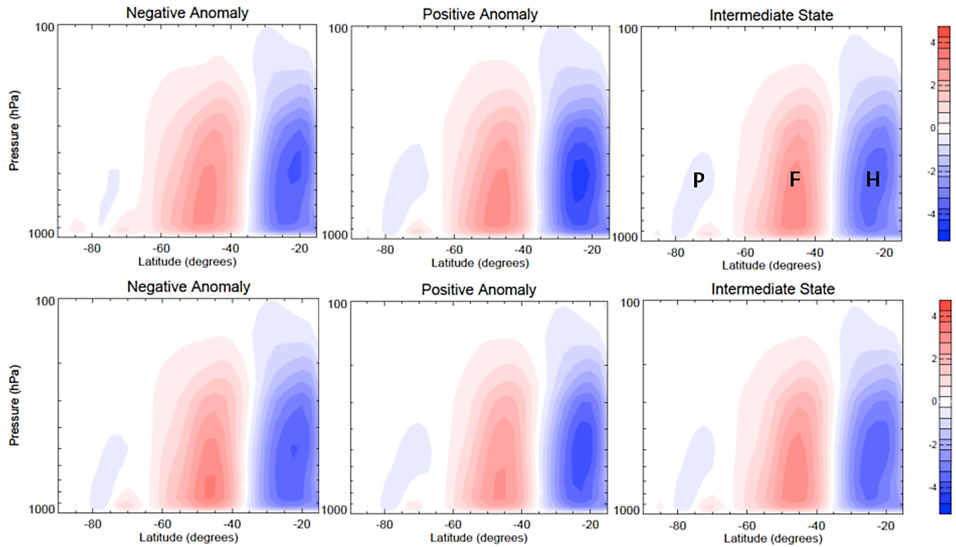

Figure 8. The deseasonalised mean meridional mass streamfunction obtained from daily mean NCEP/NCAR reanalysis (1979–2012). Shown left to right are composites for negative, positive and intermediate monthly surface pressure anomalies in the SIO region (upper three panels) and SWP region (lower three panels). Positive (negative) values denote clockwise (anticlockwise) rotation in the plane of the figure; the Hadley, Ferrel and Polar cells are marked H, F and P, respectively. The units are 10^{10} kg s^{-1}.

CC BY

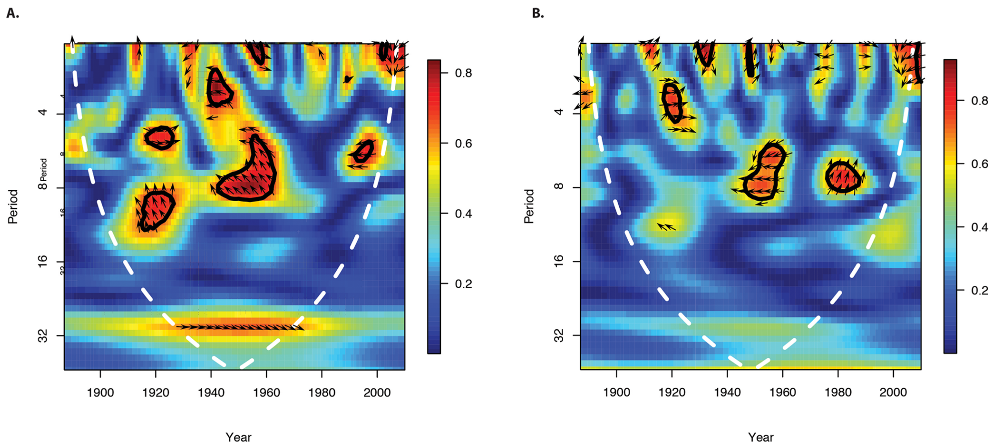

Figure 9. Wavelet coherence plots between the South Geographic Pole δD and the SIO **(a)** and SWP **(b)** deseasonalised surface pressure anomalies extracted from the 20th Century Reanalysis (Compo et al., 2011). Major periodicities (95 % confidence) are defined by solid black contours; the white dashed lines denote the cone of influence. Vectors indicate relative phase with angle measured anticlockwise from in-phase (pointing to the right) through SIO pressure leading temperature in quadrature (pointing upwards) to anti-phase (pointing left).

TCD
9, 4019–4042, 2015

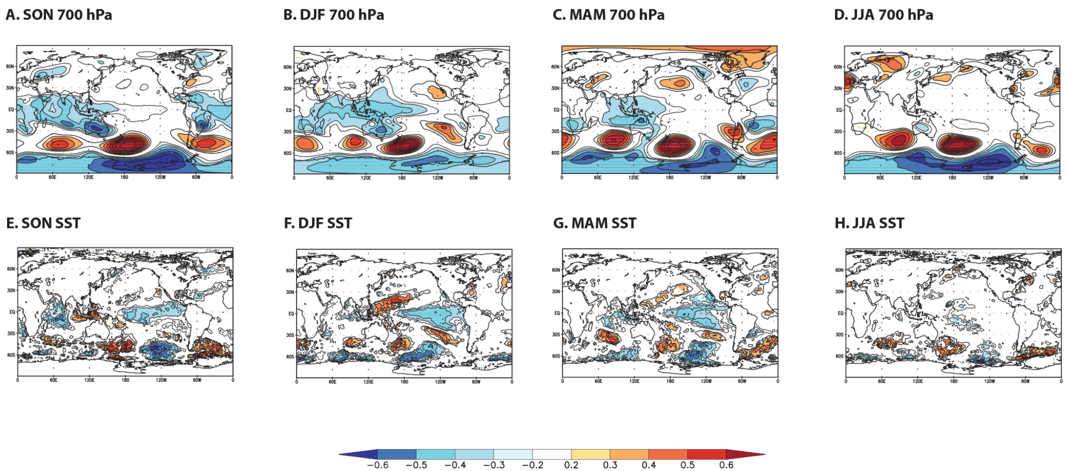

Figure 10. Seasonal correlations between Southwest Pacific (SWP) pressure (700 hPa) and geopotential height (700 hPa) **(a–d)** (Dee et al., 2011), and sea surface temperatures (SSTs) **(e–i)** (Rayner et al., 2003) (1979–2013; *p* value $< 0.1\,\%$). Note the significant inverse relationship between SWP, tropical west Pacific GPH and central and east tropical Pacific SSTs during September–November, December–February and March–May (but not June–August), a region and seasons closely associated with El Niño–Southern Oscillation (ENSO) variability (Collins et al., 2010).

TCD
9, 4019–4042, 2015

CC BY